Marina S. Leite
Varlei Rodrigues
Daniela Zanchet

Structural effects on Au and Ag colloidal nanoparticles

M.S. Leite · V. Rodrigues
D. Zanchet (✉)
Brazilian Synchrotron Light Laboratory,
Cx.P. 6192, 13084-971 Campinas,
SP, Brazil
e-mail: zanchet@lnls.br
Tel: +55-19-32874632
Fax: +55-19-3287-4520

M.S. Leite
IFGW-UNICAMP, Cx. P. 6163,
13084-971 Campinas, SP, Brazil

Abstract On the nanometer scale, size reduction effects affect materials properties. Au and Ag nanoparticles are interesting cases owing to a structural transition that occurs at nanometric sizes; this has been explored, for example, to change material properties. Here, we present structural studies on dodecanethiol-capped Au and Ag colloidal nanoparticles synthesized at room temperature and 80 °C. For the same synthesis conditions, Au nanoparticle sizes are smaller than Ag ones. From the structure point of view, the synthesis temperature has a minor effect on Au nanoparticles but it induces stacking faults and twin planes in the Ag case. These results suggest that hexagonal close-packed symmetry may be favored for Ag for certain synthesis conditions, but this has not been identified for Au.

Keywords Colloidal gold · Nanoparticle · High-resolution transmission electron microscopy · X-ray diffraction

Introduction

On the nanometer scale, size reduction effects play an important role and greatly affect material properties. In this aspect, unique properties, such as the catalytic activity and optical properties of Au nanoparticles, have been reported [1–3]. In fact, Au colloids have been known for more than a century but they have attracted special attention in the last few years owing to the improvement of synthetic methods and the development of novel applications based on their characteristic surface plasmon resonance, such as surface-enhanced Raman spectroscopy and biological labeling [2–4]. In particular, strong modifications of plasmon peaks have been found for anisotropic particles, such as nanorods and nanoprisms, increasing the potential applications of these nanosystems [3, 5, 6]. In a similar way, Ag nanoparticles have also been the subject of many studies and the development of new technologies [6].

From the structure point of view, Au and Ag are also interesting materials since a structure transition has been found for sizes below 4 nm [7]. Since the atomic arrangement affects most particle properties and it is directly related to morphology, structural modifications could be better explored to tune material properties and shape-control.

Au and Ag have the same bulk crystallographic structure (face-centered cubic, fcc, $a = 4.07$ Å) and are expected to follow similar structural modifications as a function of particle size, i.e., decahedra in the 1–3-nm range and icosahedra for sizes below 1 nm [7]. Icosahedra and decahedra are noncrystallographic structures known as multiply twinned particles and they are characterized by a fivefold axis symmetry. The origin of this structural transition is based on surface energy that becomes important at nanometric size, and that is minimized by structural modifications. The difference in energy among these structures, however, is small and a real sample usually presents more than one type of structure. Kinetic effects may also play an important role during particle formation and they have been used to produce metastable structures [8, 9]. Although several works can be found on Au nanoparticles [7, 8, 10–12], much less is known about the structure of Ag nanoparticles [8, 13].

Here, we address structural effects on Au and Ag nanoparticles produced by colloidal methods. Despite their structural similarity in bulk, Au and Ag nanoparticles have shown different structural aspects when synthesized under the same conditions. An important result is the tendency of Ag nanoparticles to present defects (stacking faults and twins), which are not observed in Au nanoparticles.

Experimental

Au and Ag nanoparticles were produced by the method developed by Brust et al. [4]. Briefly, hydrogen tetrachloroaurate or silver nitrate is reduced by sodium borohydrate in a two-phase system (water and toluene) in the presence of dodecanethiol (capping molecules). Tetra-*n*-octylammonium bromide is used as phase-transfer agent. Samples were synthesized under Ar at room temperature (Au-RT and Ag-RT, 25 °C) and at 80 °C (Au-80 °C and Ag-80 °C), keeping the other parameters constant. Size and structural characterization were performed by a combination of a local probe technique, such as high-resolution transmission electron microscopy (HRTEM), and average-type techniques, such as small-angle X-ray scattering (SAXS) and X-ray diffraction (XRD). HRTEM was performed with a JEM-3010, operating at 300 kV (1.7-Å point resolution) at the Electron Microscopy Laboratory (LME) at the Brazilian Synchrotron Light Laboratory (LNLS). SAXS experiments were performed in dilute solutions at the SAXS beamline-LNLS, with $\lambda = 1.608$ Å and $(0.01) < q < 0.7$ Å^{-1} ($q = 4\pi\sin\theta/\lambda$; q is the scattering vector, 2θ is the scattering angle and λ is the X-ray wavelength). XRD measurements were performed in dried samples either at the XRD1 beamline-LNLS ($\lambda = 1.06$ Å) or using a conventional source ($\lambda = 1.54$ Å), operating in θ–2θ geometry. XRD data were compared with simulated XRD patterns, using the Debye formula, of nanoparticles of different sizes and structures [7, 8, 10].

Results and discussion

The low-magnification TEM images of Au-RT and Ag-RT nanoparticles and the corresponding size distributions are shown in Fig. 1a. Both samples present spherical particles with average diameters (d_m) of 2.0 and 4.6 nm, respectively, and a narrow size distribution ($\sigma = 0.4$ nm). SAXS data of the same samples are presented in Fig. 2; the dashed lines correspond to theoretical scattering curves of spherical particles with a Gaussian size distribution, showing good agreement with the TEM results [Au-RT $d_m = 1.7$ nm ($\sigma = 0.34$ nm); Ag-RT $d_m = 4.0$ nm ($\sigma = 0.6$ nm)]. Increasing the synthesis temperature to 80 °C has a different effect on the Au and Ag nanoparticle size; it increases the particle size for Au ($d_m = 3.0$ nm for Au-80 °C), while it does not have a significant effect for Ag (data not shown).

Concerning the particle structure, HRTEM images have shown that all the samples present structure distributions, as mentioned before. Representative HRTEM images for the four samples (more than 100 images were analyzed for each one) are shown in Fig. 3.
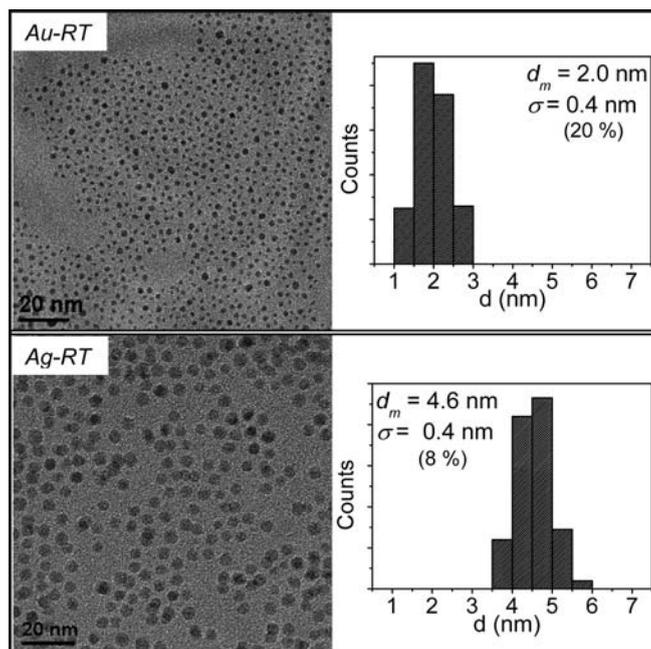

Fig. 1 *TEM* images of Au-RT and Ag-RT nanoparticles and corresponding size distributions. More than 300 particles were evaluated for each sample
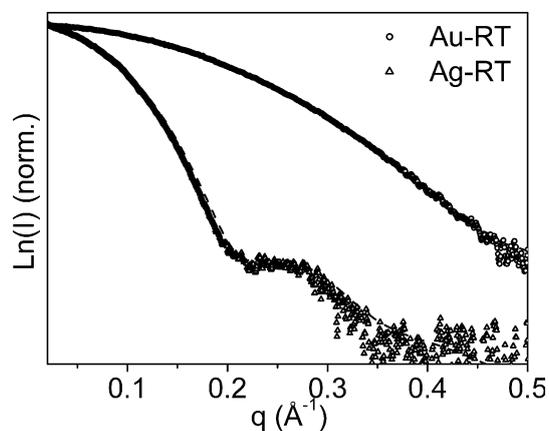
Fig. 2 Small-angle X-ray scattering data for the same samples as in Fig. 1. The *dashed lines* correspond to theoretical scattering curves of spherical particles with a Gaussian size distribution

In both the Au-RT (Fig. 3a, b) and the Au-80 °C (Fig. 3c, d) samples decahedral and fcc particles could be frequently identified. In the case of Ag-RT (Fig. 3e, f) and Ag-80 °C (Fig. 3g, h), the HRTEM images show a large number of perfect fcc particles and fcc particles with defects. In this case, however, the increase in the synthesis temperature seems to result in an increase in the number of defects per particle. This can be seen in Fig. 3 h, which shows a very defective particle with several stacking faults and twin planes. As a

Fig. 3 Representative *HRTEM* images of **a** decahedral Au-RT, **b** face-centered cubic (*fcc*) Au-RT, **c** decahedral Au-80 °C, **d** fcc Au-80 °C, **e** fcc Ag-RT, **f** fcc Ag-RT with a twin plane, **g** fcc Ag-80 °C and **h** defective fcc Ag-80 °C. Note the several stacking faults and twin planes in **h**
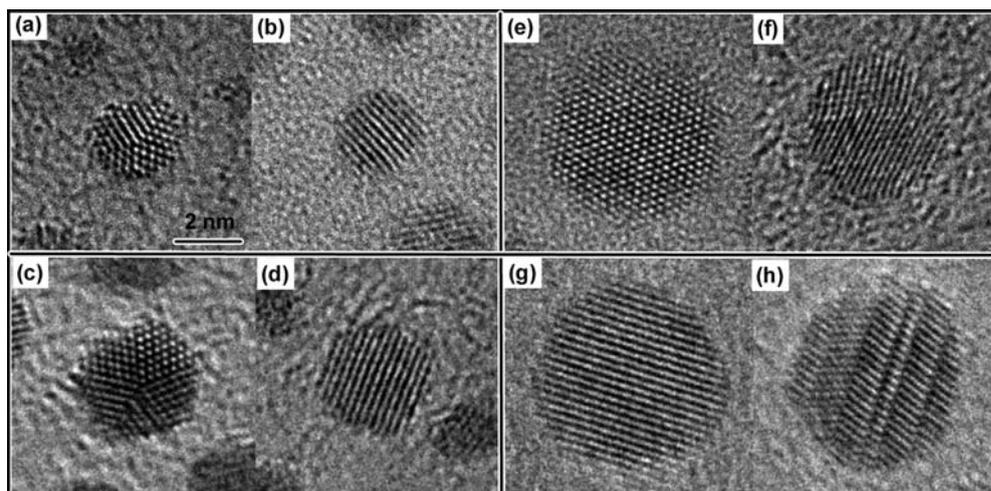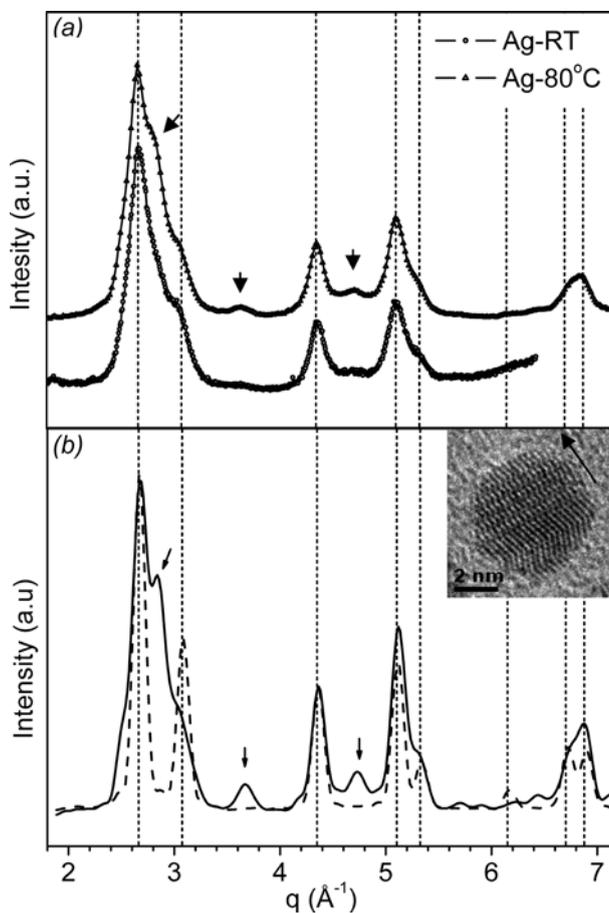
consequence, from the structural point of view the synthesis temperature seems to have more of an effect for Ag than for Au. It is important to remark that in the 2–3-nm size range a decahedron is the energetically favored structure, whereas for larger particles, fcc is the expected structure.

The XRD patterns were analyzed to confirm the HRTEM results. In the case of Au, a careful analysis of the XRD patterns (data not shown) confirms that the majority population is indeed decahedral particles for Au-RT and Au-80 °C. The decahedral pattern can be easily identified by the higher relative intensity of the (111) peak compared with the fcc pattern and the convolution of the (220) and (311) peaks [7, 10].

The XRD patterns of Ag-RT and Ag-80 °C are shown in Fig. 4. It can be seen that most of the peaks match the fcc pattern (dotted lines) and that the peak broadening is similar for both samples, confirming the close nanoparticle size. In Ag-80 °C, however, additional features at 2.8, 3.6 and 4.7 Å^{-1} can be clearly seen (marked by arrows). These features cannot be explained by fcc, decahedral or icosahedral patterns, indicating an additional type of structure. HRTEM had already pointed out the existence of defective fcc particles, mainly for the Ag-80 °C sample. A HRTEM image of a defective fcc particle (inset) and the corresponding simulated XRD pattern are shown in Fig. 4b. The dashed curve corre-

sponds to a perfect fcc particle with the same size. It can be clearly seen that the additional features that appear in the experimental XRD pattern are a consequence of stacking faults and twin planes. Looking carefully at the XRD pattern of Ag-RT, we could identify the same features, but with much lower intensity, showing that in

Fig. 4a X-ray diffraction pattern of Ag-RT and Ag-80 °C samples. The *dashed lines* correspond to the fcc peak positions. The *arrows* show additional features that are enhanced in the Ag-80 °C pattern. **b** *Inset*: HRTEM image of a defective particle found in the Ag-80 °C sample (the *arrow* indicates the hexagonal close-packed region of this particle). The graphic shows the corresponding theoretical X-ray diffraction pattern of this particle (*solid line*). Note the same additional features present in the experimental pattern, marked by arrows. The *dashed curve* corresponds to the diffraction pattern of a perfect fcc particle of the same size

the Ag case there is indeed a change in the structure distribution when the synthesis temperature is increased.

One interesting point to note is that the presence of stacking faults indicates a transition from fcc to hexagonal close-packed (hcp). In particular, the HRTEM image in the inset of Fig. 4 corresponds to a particle that is half hcp (indicated by the arrow) and half fcc with a twin plane. These results suggest that a higher synthesis temperature may enhance the hcp symmetry in Ag nanoparticles, and additional studies are under way to corroborate this point. Nevertheless, this is a very interesting result since several experiments have been reported on the Au system, and the hcp symmetry has not been identified [10–12]. A hypothesis to explain the structural differences found in Au and Ag could be based on the faster growth rate of Ag nanoparticles. Additional data, using higher synthesis temperatures, will help to address this issue. In addition, the energy stability of hcp Ag and Au particles as a function of particle size has still to be evaluated by theoretical calculations to determine whether different behavior should be expected. The hcp system is an interesting one that might be explored, for example, to induce anisotropic-type growth and produce nanorods or nanodisks with small diameters (below 10 nm).

Conclusions

Au and Ag colloidal nanoparticles have been synthesized at room temperature and 80 °C. The increase in synthesis temperature leads to larger particle sizes in the case of Au, but it does not have a significant effect on Ag. By using HRTEM in association with XRD measurements and simulations, we have been able to point out structural differences on Ag and Au colloidal nanoparticles. Whereas Au nanoparticles preferentially form decahedra at both synthesis temperatures, Ag nanoparticles have the tendency to form several stacking faults, and this is enhanced at 80 °C. The sequence of stacking faults in the fcc structure leads to a hcp structure and particles with half hcp character have been identified in the Ag-80 °C sample. These results suggest that hcp symmetry may be favored in Ag under certain synthesis conditions and additional studies are under way to address this issue.

References

1. Sanchez A et al (1999) J Phys Chem A 103:9573
2. Mulvaney P (1996) Langmuir 12:788
3. El-Sayed MA (2001) Acc Chem Res 34:257
4. Brust M et al (1994) J Chem Soc Chem Commun 801
5. Link S, El-Sayed, MA (1999) J Phys Chem B 103:8410
6. Jin R et al (2001) Science 294:1901
7. Hall BD (2000) J Appl Phys 87:1666, and references therein
8. Murray CB, Kagan CR, Bawendi MG (2000) Annu Rev Mater Sci 30:545
9. Dinega DP, Bawendi MG (1999) Angew Chem 38:1788
10. Zanchet D, Hall BD, Ugarte D (2000) J Phys Chem B 104:11013
11. Whetten RL et al (1996) Adv Mater 8:428
12. Vogel W et al (1999) J Phys Chem B 102:10853
13. Baletto F, Mottet C, Ferrando R (2000) Phys Rev Lett 84:5544